



HAL
open science

Studies on DNA binding properties of new Schiff base ligands using spectroscopic, electrochemical and computational methods: Influence of substitutions on DNA-binding

Arezoo Jamshidvand, Mehdi Sahihi, Valiollah Mirkhani, Majid Moghadam, Iraj Mohammadpoor-Baltork, Shahram Tangestaninejad, Hadi Amiri Rudbari, Hadi Kargar, Reza Keshavarzi, Sajjad Gharaghani

► To cite this version:

Arezoo Jamshidvand, Mehdi Sahihi, Valiollah Mirkhani, Majid Moghadam, Iraj Mohammadpoor-Baltork, et al.. Studies on DNA binding properties of new Schiff base ligands using spectroscopic, electrochemical and computational methods: Influence of substitutions on DNA-binding. *Journal of Molecular Liquids*, 2018, 253, pp.61-71. 10.1016/j.molliq.2018.01.029 . hal-04086078

HAL Id: hal-04086078

<https://hal.science/hal-04086078>

Submitted on 1 May 2023

HAL is a multi-disciplinary open access archive for the deposit and dissemination of scientific research documents, whether they are published or not. The documents may come from teaching and research institutions in France or abroad, or from public or private research centers.

L'archive ouverte pluridisciplinaire **HAL**, est destinée au dépôt et à la diffusion de documents scientifiques de niveau recherche, publiés ou non, émanant des établissements d'enseignement et de recherche français ou étrangers, des laboratoires publics ou privés.

Studies on DNA binding properties of new Schiff base ligands using spectroscopic, electrochemical and computational methods: Influence of substitutions on DNA-binding

Arezoo Jamshidvand ^a, Mehdi Sahihi ^a, Valiollah Mirkhani ^a, Majid Moghadam ^a, Iraj Mohammadpoor-Baltork ^a, Shahram Tangestaninejad ^a, Hadi Amiri Rudbari ^a, Hadi Kargar ^b, Reza Keshavarzi ^a, Sajjad Gharaghani ^c

Department of Chemistry, University of Isfahan, Isfahan 81746-73441, Iran

Department of Chemistry, Payame Noor University, Tehran, Iran

Laboratory of Bioinformatics and Drug Design (LBD), Institute of Biochemistry and Biophysics, University of Tehran, Tehran, Iran

Abstract

In this work, five new Schiff base ligands were synthesized and characterized by ¹H NMR, ¹³C NMR, FT-IR, UV-Vis and elemental analysis (CHN). L¹, L² and L³, were derived from condensation of 2-Hydroxy-5-bromobenzaldehyde with 4-aminobenzoic acid, 3-aminobenzoic acid and 3-amino-4-methylbenzoic acid with 1:1 M ratio, respectively. While, L⁴ and L⁵ were prepared from condensation of 4-aminobenzoate with 3-ethoxy-2-hydroxybenzaldehyde and 3-methoxy-2-hydroxybenzaldehyde with 1:1 M ratio, respectively. Furthermore, the crystal structure of L⁴ and L⁵ were determined by single crystal X-ray analysis. The interaction of Schiff base ligands with fish sperm DNA (FS-DNA) was investigated under physiological conditions using fluorescence quenching, UV-Vis spectroscopy, molecular docking and molecular dynamics (MD) simulation methods. The estimated binding constants (k_b) for the DNA-Ligands complexes were 8.9 × 10⁴ M⁻¹, 6.8 × 10⁴ M⁻¹, 1.2 × 10⁵ M⁻¹, 2.3 × 10⁵ M⁻¹, 1.7 × 10⁵ M⁻¹ for L¹, L², L³, L⁴ and L⁵, respectively. Based on similarity of the ligands structures and their K_b values, their affinity for binding to FS-DNA follow as: L³ > L¹ > L² and L⁴ > L⁵. The results revealed that ligands with stronger electron donating substituents, have higher DNA-binding ability than the others. Also, molecular docking results show that all of the synthesized ligands are minor groove binders and H-bond interactions have dominant role in the stability of ligand-DNA complexes.

Keywords

Schiff base ligands

Crystal structure

DNA binding

Molecular docking

Molecular dynamics simulation

1. Introduction

Cancer is a large family of diseases that involves abnormal cell growth with potential to invade or spread to the other parts of the body. Nowadays, these sorts of diseases are known as the main cause of worldwide death. However, it can be treated by disordering the DNA of cancer cells. Schiff base ligands are significant compounds which biochemists are focusing on their design and synthesis as anticancer and play an impressive role in human welfare. These compounds are the urgent ligands in modern coordination and medicinal chemistry [[1], [2], [3], [4], [5], [6], [7]]. Schiff bases are derived by substitution aldehyde/ketone with

a primary amine. The azomethine (HC N) linkage present in Schiff base ligands demonstrate a wide range of medicinal activities such as antibacterial [8, 9], antifungal [10], herbicidal, anti-inflammatory [7], anticancer, anti-diabetic [11] and antitumor [12] activities. The interaction between Schiff base ligands and DNA is one the most essential step to design and synthesis of new pharmaceutical molecules, due to the importance of DNA as the main target for anticancer drugs [13, 14]. There are three possible ways for interaction of the drugs and DNA: (i) electrostatic binding between cation species and negative charged DNA phosphate residues (ii) interaction with grooves of DNA by hydrogen bond or van der Waals interactions, and (iii) intercalative binding [[15], [16], [17]].

Recently, we have focused on designing and synthesis of novel Schiff base ligands, and investigation of their assembly with metals as well as their biological activities [[18], [19], [20]]. Herein, five new Schiff base ligands were synthesized and characterized by various spectroscopic techniques such as FT-IR, ¹H NMR, ¹³C NMR and elemental analysis (CHNS). Also, the molecular structures of two ligands were determined by single crystal X-ray diffraction technique. Furthermore, DNA binding of the synthesized Schiff base ligands was investigated using fluorescence quenching, UV-Vis spectroscopy, circular dichroism (CD), cyclic voltammetry, molecular docking and molecular dynamics simulation methods. The effect of substituents on the Schiff base ligands on their DNA-binding ability was also investigated.

2. Experimental

2.1. Chemicals and instrumentation

Fish sperm DNA (FS-DNA), *tris*(hydroxymethyl)aminomethane (Tris), ethidium bromide (3,8-diamino-5-ethyl-6-phenylphenanthridinium bromide, EB), 4-aminobenzoic acid, 3-aminobenzoic acid, 3-amino-4-methylbenzoic acid and 3-ethoxy-2-hydroxybenzaldehyde were purchased from Sigma-Aldrich. 2-Hydroxy-5-bromobenzaldehyde, 3-methoxy-2-hydroxybenzaldehyde, Sodium bicarbonate, sulfuric acid, methanol, ethanol and DMF were obtained from Merck Co. and used without further purification. All of the solutions were used freshly after preparation. The FT-IR spectra were recorded on a JASCO, FT/IR-6300 spectrometer (4000–400 cm⁻¹) as KBr pellets. The ¹H and ¹³C NMR spectra were recorded on a Bruker Avance III 400 spectrometer using CDCl₃ and DMSO-*d*₆ as solvents for Schiff base ligands. The elemental analysis was performed on Leco, CHNS-932 and Perkin-Elmer 7300 DV elemental analyzers. The UV-Vis spectra were recorded on a JASCO V-670 spectrophotometer. Fluorescence measurements were carried out on Shimadzu RF-5000 spectrofluorometer at room temperature. The cyclic voltammetry measurements (CV) were performed using an Autolab (PGSTAT 30), with a three-electrode

system: a 0.10-cm-diameter Glassy carbon (GC) disc as working electrode, a calomel electrode as reference electrode, and a Pt wire as counter electrode.

The circular dichroism (CD) spectra were recorded using Aviv spectropolarimeter model 215 (ProterionCorp., USA) at 25 °C. The scan speed was 20 nm min⁻¹. The circular dichroism (CD) spectra were recorded using 0.1 cm quartz cell in far- and near-UV region (215–310) for DNA to clarify the its structural changes during the interaction with the ligand. The CD spectra of DNA solutions were recorded before and after addition of the ligand with the most binding affinity with molar ratio of 1:1.

2.2. Preparation of ligands

2.2.1. Synthesis of L¹

2-Hydroxy-5-bromobenzaldehyde (4.02 g, 20 mmol) was added to an ethanolic solution (50 mL) of 4-aminobenzoic acid (2.75 g, 20 mmol) and the mixture was refluxed for 1 h. The yellow precipitates of L¹ were collected by filtration, washed with ethanol and then dried under vacuum at room temperature. Yield 5.31 g (83%). *Anal. Calc.* for C₁₄H₁₀BrNO₃: C, 52.53; H, 3.15; N, 4.38. Found: C, 52.51; H, 3.17; N, 4.40%. IR (KBr, cm⁻¹): ν_{asym} (COO⁻) 1680, ν_{sym} (COO⁻)

1428, ν (C—N) 1595, ν (C—N) 1279.

¹HNMR (DMSO-*d*₆, 400 MHz, 298 K) δ /ppm: 12.97 (br, 1H, OH); 12.63 (s, 1H, OH), 8.96 (s,

1H, N—CH); 8.02 (d, ³*J* = 8.8 Hz, 2H), 7.92 (d, ⁴*J* = 2.4 Hz, 1H), 7.59

(dd, ³*J* = 8.8 Hz, ⁴*J* = 2.4 Hz, 1H), 7.48 (d, ³*J* = 8.8 Hz, 2H), 6.98 (d, ³*J* = 8.8 Hz, 1H). ¹³CNMR (DMSO-*d*₆, 100 MHz, 298 K) δ /ppm: 166.79, 162.95, 159.23, 138.44, 135.96, 133.77, 131.17, 130.71, 130.42, 128.96, 121.52, 119.12, 112.49, 110.08.

2.2.2. Synthesis of L²

2-Hydroxy-5-bromobenzaldehyde (4.02 g, 20 mmol) was added to an ethanolic solution (50 mL) of 3-aminobenzoic acid (2.75 g, 20 mmol) and the mixture was refluxed for 1 h. The yellow precipitates of L² were collected by filtration, washed with ethanol and then dried in vacuum at room temperature. Yield 5.12 g (80%). *Anal. Calc.* for C₁₄H₁₀BrNO₃: C, 52.53; H, 3.15; N, 4.38. Found: C, 52.50; H, 3.18; N, 4.35%. IR (KBr, cm⁻¹): ν_{asym} (COO⁻) 1677, ν_{sym} (COO⁻) 1421,

ν (C—N) 1619, ν (C—N) 1274.

¹HNMR (DMSO-*d*₆, 400 MHz, 298 K) δ /ppm: 13.19 (br, 1H, OH); 12.80 (s, 1H, OH), 9.01 (s,

1H, N—CH); 7.93 (d, ⁴*J* = 2.4 Hz, 2H), 7.89 (dt, ³*J* = 7.6 Hz, ⁴*J* = 1.2 Hz, 1H), 7.65

(dt, ³*J* = 7.6 Hz, ⁴*J* = 1.2 Hz, 1H), 7.61 (d, ³*J* = 8.0 Hz, 1H), 7.58 (dd, ³*J* = 8.8 Hz, ⁴*J* = 2.4 Hz, 1H), 6.97 (d, ³*J* = 8.8 Hz, 1H). ¹³CNMR (DMSO-*d*₆, 100 MHz, 298 K) δ /ppm: 166.84, 162.69, 159.23, 148.29, 135.70, 133.98, 132.12, 129.79, 127.78, 126.17, 121.65, 121.21, 119.04, 109.98.

2.2.3. Synthesis of L³

2-Hydroxy-5-bromobenzaldehyde (4.02 g, 20 mmol) was added to an ethanolic solution (50 mL) of 3-amino-4-methylbenzoic acid (3.02 g, 20 mmol) and the mixture was refluxed for 1 h. The yellow precipitates of L³ were collected by filtration, washed with ethanol and then dried in vacuum at room temperature. Yield 5.68 g (85%). *Anal. Calc.* for C₁₅H₁₂BrNO₃: C, 53.91; H, 3.62; N, 4.19. Found: C, 53.95; H, 3.65; N, 4.20%. IR (KBr, cm⁻¹): ν_{asym} (COO⁻) 1683,

ν_{sym} (COO⁻) 1422, ν (C—N) 1611, ν (C—N) 1279.

^1H NMR (DMSO-*d*₆, 400 MHz, 298 K) δ /ppm: 13.06 (s, 2H, OH), 8.96 (s, 1H, N-CH); 7.97 (d, $^4J=2.4$ Hz, 1H), 7.85 (d, $^4J=1.6$ Hz, 1H), 7.80 (dd, $^3J=7.6$ Hz, $^4J=1.6$ Hz, 1H), 7.58 (dd, $^3J=8.8$ Hz, $^4J=2.4$ Hz, 1H), 7.45 (d, $^3J=7.6$ Hz, 1H), 6.97 (d, $^3J=8.8$ Hz, 1H), 2.50 (s, 3H). ^{13}C NMR (DMSO-*d*₆, 100 MHz, 298 K) δ /ppm: 166.94, 162.32, 159.38, 147.00, 137.23, 135.69, 134.14, 130.82, 129.88, 127.66, 121.28, 119.01, 118.71, 109.93, 17.92.

For synthesis of L⁴ and L⁵ ligands, 4-aminobenzoic acid was converted to 4-aminobenzoate according to the following procedure:

4-Aminobenzoic acid (2.75 g, 20 mmol) was dissolved in MeOH (100 mL) and refluxed in the presence of 3 mL concentrated sulfuric acid for 4 h. After the reaction was completed, the solution was concentrated to approximately 10 mL and neutralized by adding NaHCO₃ aqueous solution (10%). The crude crystal was filtered and recrystallized from MeOH/H₂O (1/1) to obtain the methyl 4-aminobenzoate (yield 63%) [21].

2.2.4. Synthesis of L⁴

3-Ethoxy-2-hydroxybenzaldehyde (3.32 g, 20 mmol) was added to an ethanolic solution (50 mL) of 4-aminobenzoate (3.02 g, 20 mmol) and the mixture was refluxed for 1 h. The resultant red solution was filtered. Red single crystals of the title compound were re-crystallized from methanol by slow evaporation of the solvents at room temperature over several days. Yield 4.96 g (83%). *Anal.* Calc. for C₁₇H₁₇NO₄: C, 68.22; H, 5.72; N, 4.68. Found: C, 68.19.51; H,

5.74; N, 4.66%. IR (KBr, cm⁻¹): ν_{asym} (COO⁻) 1706, ν_{sym} (COO⁻) 1455, ν (C-N) 1591, ν (C-N) 1278.

^1H NMR (CDCl₃, 400 MHz, 298 K) δ /ppm: 13.39 (s, 1H, OH), 8.67 (s, 1H, N-CH); 8.12 (d, $^3J=8.4$ Hz, 2H), 7.33 (d, $^3J=8.4$ Hz, 2H), 7.06 (dd, $^3J=7.6$ Hz, $^4J=1.2$ Hz, 2H), 6.91 (d, $^3J=8.0$ Hz, 1H), 4.17 (q, $^3J=7.2$ Hz, 2H, -CH₂-CH₃); 3.95 (s, 3H, -OCH₃); 1.53 (t, $^3J=7.2$ Hz, 3H, CH₃-CH₂-). ^{13}C NMR (DMSO-*d*₆, 100 MHz, 298 K) δ /ppm: 166.57, 164.22, 152.21, 151.46, 148.49, 131.60, 131.06, 128.40, 124.05, 121.200, 118.86, 118.84, 115.20, 113.78, 56.20, 52.23.

2.2.5. Synthesis of L⁵

3-Methoxy-2-hydroxybenzaldehyde (3.04 g, 20 mmol) was added to an ethanolic solution (50 mL) of 4-aminobenzoate (3.02 g, 20 mmol) and the mixture was refluxed for 1 h. The resultant red solution was filtered. Red single crystals of the title compound were re-crystallized from methanol by slow evaporation of the solvents at room temperature over several days. Yield 4.62 g (81%). *Anal.* Calc. for C₁₆H₁₅NO₄: C, 67.36; H, 5.30; N, 4.91. Found: C, 67.39; H, 5.35;

N, 4.90%. IR (KBr, cm⁻¹): ν_{asym} (COO⁻) 1721, ν_{sym} (COO⁻) 1467, ν (C-N) 1591, ν (C-N) 1261.

^1H NMR (CDCl₃, 400 MHz, 298 K) δ /ppm: 13.31 (s, 1H, OH), 8.65 (s, 1H, N-CH), 8.11 (d, $^3J=8.4$ Hz, 2H), 7.32 (d, $^3J=8.4$ Hz, 2H), 7.05 (dd, $^3J=8.0$ Hz, $^4J=1.2$ Hz, 2H), 6.92

(d, $^3J=8.0$ Hz, 1H), 3.95 (s, 3H, OCH₃), 3.94 (s, 3H, OCH₃). ^{13}C NMR (DMSO-*d*₆, 100 MHz, 298 K) δ /ppm: 166.54, 164.15, 152.09, 151.71, 147.74, 131.05, 128.36, 124.09, 121.15, 118.95, 118.79, 116.65, 64.61, 52.21, 14.89.

2.3. Single crystal diffraction studies

X-ray data for L⁴ and L⁵ were collected on a STOE IPDS-II diffractometer with graphite monochromated Mo K α radiation. The suitable crystals were chosen using a polarizing microscope and were mounted on a glass fiber which were used for data collection. Data were collected at 298(2) K in a series ω scans in 1° oscillations and integrated using the StoeX-AREA [22] software package. A numerical absorption correction was applied using the X-RED [23] and X-SHAPE [24] software for the ligands. The data were corrected for Lorentz and Polarizing effects. The structures were solved by direct methods using SIR2004. The non-hydrogen atoms were refined anisotropically by the full-matrix least-squares method on F^2 using SHELXL [25]. All hydrogen atoms were added at ideal positions and constrained to ride on their parent atoms. Crystallographic data are listed in Table 1. Selected bond distances and angles are summarized in Table S1.

Table 1. Crystal data and refinement parameters for L⁴, L⁵.

Empirical formula	C₁₇H₁₇NO₄(L⁴)	C₁₆H₁₅NO₄ (L⁵)
Formula weight	299.33	285.29
Crystal system, space group	Monoclinic, P 21/c	Orthorhombic, P 21 21 21
<i>a</i> [Å]	6.9376 (14)	4.7539 (10)
<i>b</i> [Å]	12.927 (3)	12.482 (3)
<i>c</i> [Å]	16.983 (3)	23.662 (5)
α	90	90
β	90.47 (3)	90
γ	90	90
<i>V</i> [Å³]	1523.0 (5)	1404.0 (5)
<i>Z</i>	4	4
<i>Calculated density</i> [Mg/m³]	1.305	1.350
<i>Absorption coefficient</i> [mm⁻¹]	0.093	0.098
<i>F</i>(000)	632	600
Index ranges	-8 ≤ <i>h</i> ≤ 8	-5 ≤ <i>h</i> ≤ 5

Empirical formula	C ₁₇ H ₁₇ NO ₄ (L ⁴)	C ₁₆ H ₁₅ NO ₄ (L ⁵)
	-15 ≤ k ≤ 15	-14 ≤ k ≤ 13
	-20 ≤ l ≤ 20	-28 ≤ l ≤ 28
Theta range for data collection	2.870 to 24.999	3.055 to 24.999
Reflections collected	9354	9007
Independent reflections	[R(int) = 0.2958]2687	2471 [R(int) = 0.0697]
Data completeness	99.9%	99.7%
Refinement method	Full-matrix least-squares on F ²	Full-matrix least-squares on F ²
Data/restraints/parameters	2687/o/202	2471/0/194
Goodness-of-fit on F²	0.801	0.887
Final R indices [I > 2σ (I)]	R ₁ = 0.1545 WR ₂ = 0.3331	R ₁ = 0.0340 WR ₂ = 0.0746
R indices (all data)	R ₁ = 0.2128 WR ₂ = 0.3554	R ₁ = 0.0486 WR ₂ = 0.0785
Largest diff. peak and hole	0.390 and -0.631 e.Å ⁻³	0.121 and -0.164 e.Å ⁻³

2.4. DNA binding studies

2.4.1. Preparation of the ligands and DNA stock solutions

The stock solution of FS-DNA was prepared in 50 mM Tris buffer at pH = 7.5 and was stored at 4 °C. The FS-DNA concentration per nucleotide was determined using absorption intensity at 260 nm after adequate dilution with the buffer and using the reported molar absorptivity of 6600 M⁻¹.cm⁻¹ [26]. Purity of FS-DNA solution was confirmed by ratio of UV absorbance at 260 and 280 nm (A₂₆₀/A₂₈₀ = 1.9), indicating that FS-DNA is free from protein impurity [27]. Also, the stock solutions of the ligands were prepared in dimethylformamide (DMF) and then was diluted to the desired concentrations with corresponding buffer. The volume of DMF in all final solutions were <0.5% (v/v), so the effect of DMF was negligible.

2.4.2. Fluorescence spectroscopy measurements

Fluorescence spectroscopy is a sensitive and effective method to study binding of drugs to biomacromolecules. Fluorescence quenching experiment can help us to obtain the binding mode, binding constants, number of binding sites and intermolecular distances [28]. The interactions of DNA with the synthesized Schiff base ligands were investigated using fluorescence quenching experiment. Quartz cuvette with 1 cm optical path length was used and the excitation and emission slits were set at 5 and 10 nm, respectively. To investigate the binding of the ligands with DNA, the FS-DNA solution was stirred with ethidium bromide (EB) with molar ratio of DNA:EB 10:1 for 1 h at 4 °C. Significant increase of fluorescence intensity of EB is observed at the presence of FS-DNA due to intercalation of the EB molecules into the double helix of DNA [[29], [30], [31], [32]]. Then, various amounts of the ligands (0–250 µM) were added to this mixture. The fluorescence spectra were recorded in the range of 500–700 nm with excitation wavelength of 520 nm. The mixture was allowed to incubate for 2 min after addition of the ligands.

Moreover, in all of the DNA binding experiments, the measured fluorescence intensities were corrected for the dilution and the inner filter effect.

2.4.3. UV–Vis absorption spectroscopy measurements

Electronic absorption spectroscopy is one of the used methods for studying the binding affinity. To confirm the binding of the ligands to DNA, absorption titration experiments were carried out at room temperature. The UV–Vis absorption spectra of the ligands solutions (10 µM) in the absence and presence of various amounts of FS-DNA (0–50 µM) were recorded. In all of the measurements, the mixture was allowed to incubate for 2 min before recording the related spectra. Absorption curves of ligands–DNA mixtures were corrected for both absorption of DNA solutions and the dilution effect.

2.4.4. Molecular docking procedure

Studying the interaction between drug molecules and biomacromolecules, is one of the interesting topics in biochemistry [33]. Molecular docking is one of the known theoretical techniques for prediction of interaction between drugs and biomacromolecules. To dock our ligands to DNA, The 3D structures of the L⁴ and L⁵ ligands was generated using the .cif file of their X-ray crystal structures. The .cif files were converted to the .pdb format using the Mercury software (<http://www.ccdc.cam.ac.uk/>). The geometry of the L¹, L², L³ ligands were optimized using Gaussian 03 [34] at the level of B3LYP/6-31G** [35, 36]. The crystal structure of DNA (PDB ID: 423D) with sequence d(ACCGACGTCGGT)₂ were taken from the Brookhaven Protein Data Bank (<http://www.rcsb.org/pdb>). The resolution of this file was 1.6 Å. Water molecules were deleted from the .pdb files and missing hydrogen atoms were added. Flexible-ligand docking was carried out by AutoDock 4.2.5.1 molecular docking program using the implemented empirical free energy function and the Lamarckian Genetic Algorithm (LGA) [37]. The Gasteiger charges were added to the macromolecule input file and the AutoGrid was used to calculate grids. For docking of the synthesized ligands to DNA, in first step a blind docking with 126 lattice points along X, Y, and Z axes was performed to find the binding site of complexes on DNA with a grid point spacing of 0.375 Å. In the next step, the centre of the grid box was located at the binding site and the second docking was performed using a cubic box with

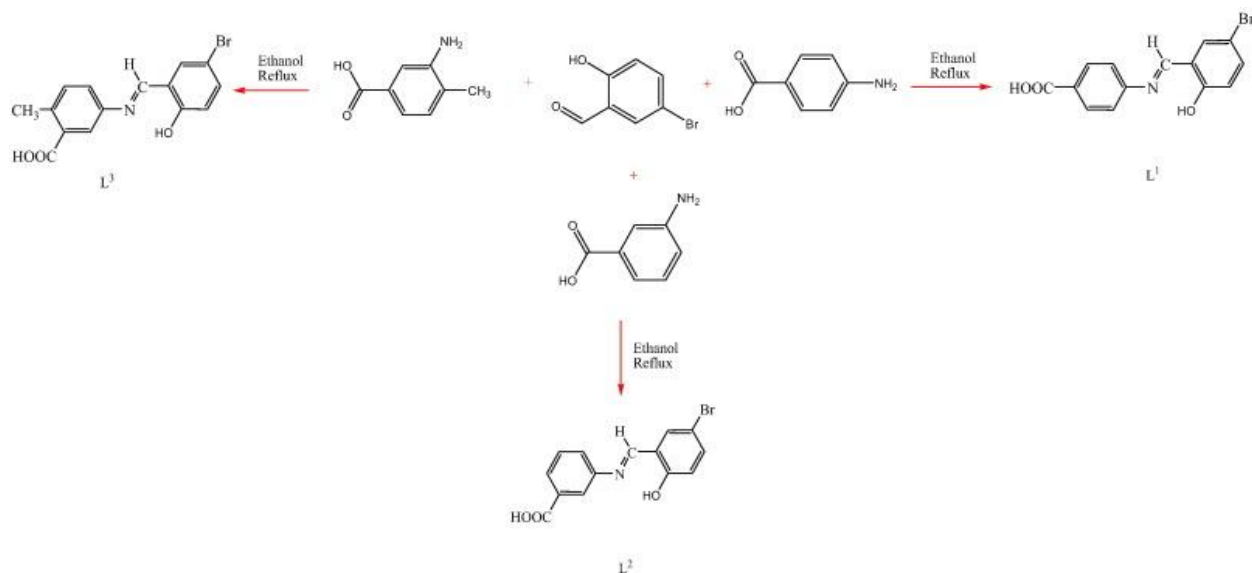
60 × 60 × 60 dimensions. 250 docking runs with 25,000,000 energy evaluations for each run were performed.

2.4.5. Molecular dynamics (MD) simulation

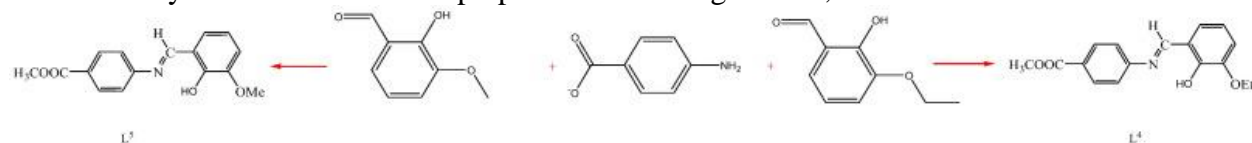
MD simulation method was used to compare the structural changes of DNA in the absence and presence of the ligands. The Schiff base-DNA complexes with the most negative free binding energy were considered as the initial conformations for the MD studies. GROMACS 5.1.2 package [38] and Amber99 force field [39, 40] were used to carry out all MD studies. The partial atomic charges of the ligands were calculated using Gaussian 03 [41] at the level of B3LYP [42], while the other intramolecular force-field parameters were generated with ACPYPE [43]. Free DNA and Schiff base-DNA complexes were located in the cubic box with the periodic boundary conditions in the three directions. The solutes were placed in the centre of box and the minimum distance between solute surface and the box was 1.0 nm. The box was filled with TIP3P water molecules [44, 45], and the solvated systems were neutralized by adding appropriate amounts of sodium ions (Na⁺) and chloride ions (Cl⁻). After energy minimization using the steepest descent method, the systems were equilibrated for 200 ps at the temperature of 300 K. Finally, a 10 ns MD simulation was carried out at 1 bar and 300 K. Parrinello-Rahman barostate [46, 47] at 1 bar, Berendsen thermostat [48] at 300 K. 9 Å cut off for Van der Waals (VdW) and Coulomb interactions and the particle mesh Ewald (PME) method [49, 50] for long range electrostatics were used. The leap-frog algorithm with the 2 fs time step was used to integrate the equation of motions. Finally, an all-bond constrain was used to keep the ligands from drifting and the atomic coordinates were recorded to the trajectory file every 0.5 ps for later analysis.

3. Result and discussion

o-Hydroxy Schiff-bases ligands are an important class of compounds from crystallography and biological activity points of view mostly because of their intramolecular hydrogen bonds. The *o*-Hydroxy ligands synthesized in this work are stable in air for an extended period of time and are soluble in the most common solvents such as methanol, ethanol, DMF, chloroform and DMSO. Scheme 1, Scheme 2 present the synthetic procedure of these ligands. The ligands were characterized by FT-IR, ¹H and ¹³C NMR spectroscopies. Moreover, the structures of L⁴ and L⁵ were determined by single crystal X-ray analysis. Analytical and physical data of Schiff base ligands are listed in Table 3.



Scheme 1. Synthetic routes for the preparation of the ligands L¹, L² and L³.



Scheme 2. Synthetic routes for the preparation of the ligands L⁴ and L⁵.

3.1. IR spectra

The most characteristic feature in the **IR** spectra of the Schiff base ligands comes from the **C N stretching vibrations**. In the FT-IR spectra of these ligands, the stretching vibration

of **imine** group (C N) appeared at 1595, 1619, 1611, 1591 and 1591 cm^{-1} for L¹, L², L³, L⁴ and L⁵ ligands, respectively that confirmed the synthesis of Schiff bases. The strong band

related to the C O stretching were observed at the region of 1279, 1274, 1279, 1278 and 1261 cm^{-1} for L¹, L², L³, L⁴ and L⁵ ligands, respectively. In the same way, the bands at 1680, 1677, 1683, 1706, 1721 cm^{-1} , attributed to COO⁻ (asymmetric) and the bands at 1428, 1421, 1422, 1455 and 1467 cm^{-1} assigned to the COO⁻ (symmetric) stretching vibrations for L¹, L², L³, L⁴ and L⁵ ligands, respectively confirmed the successful synthesis of these ligands. The presence of several medium intensity bands at 2800–3100 cm^{-1} in FT-IR spectra of ligands suggests the

existence of C H stretching vibrations of aliphatic and aromatic protons. In Table 4 characteristic IR stretching bands of Schiff base ligands are listed.

3.2. NMR spectra

The ^1H and ^{13}C NMR spectra were run in DMSO- d_6 (for L^1 , L^2 , L^3) and CDCl_3 (for L^4 and L^5) and gave the expected simple spectra, indicating the integrity of the Schiff base ligands. The spectra obtained after 12, 24 and 120 h were similar to the initial spectra indicating that the Schiff base ligands are stable in solution.

The ^1H NMR spectrum of the L^1 in DMSO- d_6 showed the aromatic protons as a multiplet in the range of 6.97 – 8.03 ppm. The OH protons of the phenolic and carboxylic acid groups are appeared at 12.63 ppm and 12.97 ppm, respectively. The imine proton was appeared as a sharp singlet at 8.96 ppm (Fig. S1 (a)).

The ^1H NMR spectrum of L^2 in DMSO- d_6 showed the singlet peak of the imine proton at 9.01 ppm. The signal observed at 12.80 ppm is assigned to OH proton of the phenolic group and OH proton of the COOH group was appeared at 13.19 ppm. The aromatic protons were observed as a multiplet at region 6.96–7.93 ppm (Fig. S2 (a)).

In the ^1H NMR spectrum (Fig. S3 (a)) of the L^3 , the aliphatic protons of the ligand are in 2.50–2.51 ppm. The aromatic protons were appeared as a multiplet in the range of 6.96–7.97 ppm and the OH protons of the phenolic and COOH groups are in the range of 13.06 ppm. The imine proton was appeared as a sharp singlet at 8.96 ppm.

The ^1H NMR spectra (Figs. S4 and S5 (a)) of L^4 and L^5 in CDCl_3 showed signal of the imine

protons (CH=N) were appeared at 8.67 and 8.65 ppm, respectively. In these ligands, the signals observed at 13.39 and 13.31 ppm are assigned to OH proton of the phenolic groups of L^4 and L^5 , respectively. The aromatic protons were observed as multiplets at 6.88–8.13 and 6.90–8.12 ppm while the aliphatic protons of the L^4 and L^5 ligands are in the range of 1.51–4.20 and 3.94–3.95 ppm, respectively.

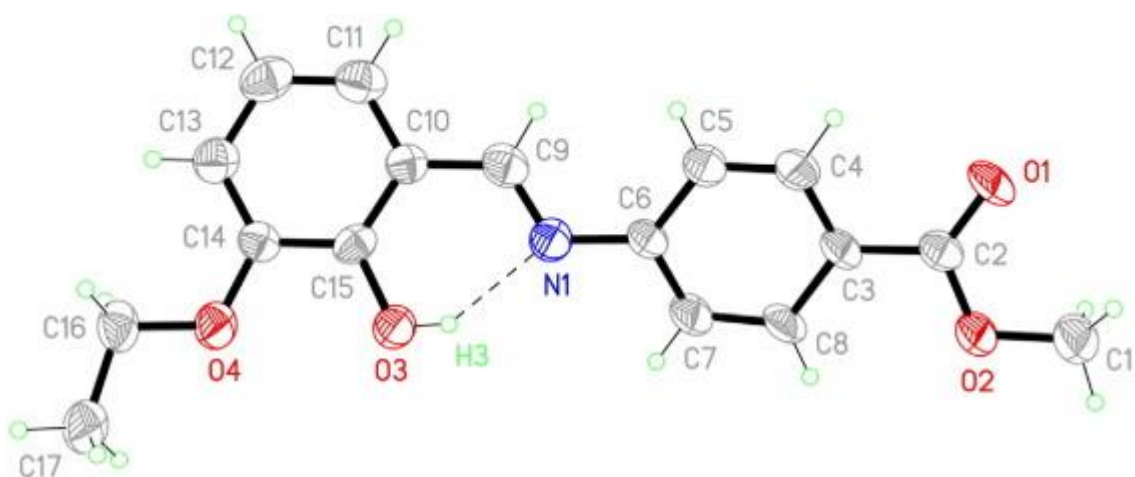
The ^{13}C NMR spectra of the ligands are consistent with the number of carbons in their structures (Figs. S1–S5. (b)). The peaks observed at 166.79, 166.84, 166.94, 166.57 and 166.54 ppm are ascribed to the imine carbon atoms of L^1 , L^2 , L^3 , L^4 and L^5 , respectively. The existence of these peaks in the spectra of ligands supports the presence of the Schiff base in them.

3.3. Description of the crystal structure of L^4 , L^5

The formation of L^4 and L^5 ligands was confirmed by single crystal X-ray diffraction analysis. Crystallographic data are collected in Table 1. Also, the selected bond lengths and angles are listed in Table S1. The L^4 and L^5 ligands crystallize in space groups $P2_1/c$ and $P2_12_12_1$, respectively and their representative ORTEP view with the atom-numbering scheme are presented in (Fig. 1) As seen in these figures, L^4 and L^5 have adopted *E*-configuration about the

C(9)–N(1) double bond with a C6–N1–C9–C10 torsion angle of 178.88° and 178.91° , respectively.

(a)



(b)

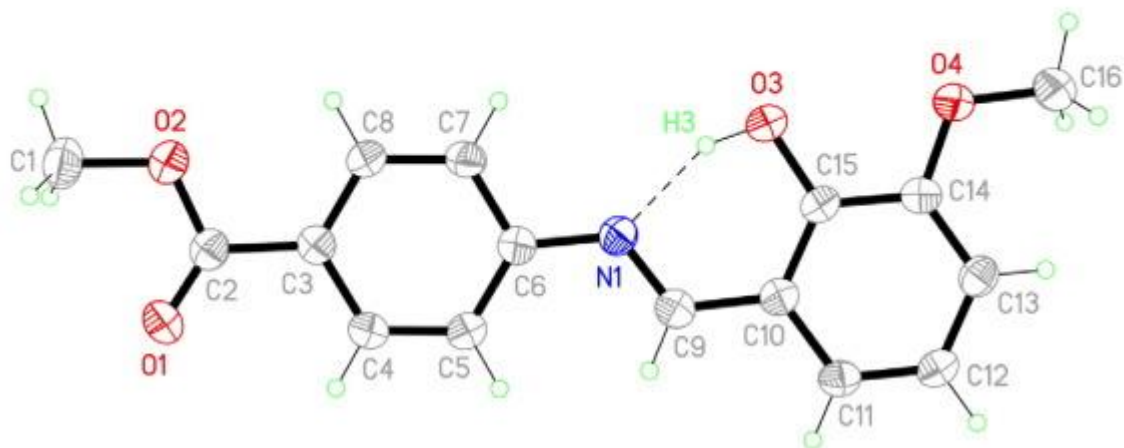


Fig. 1. a) ORTEP representation of L⁴. Displacement ellipsoids are drawn at the 30% probability level and H atoms are shown as small spheres of arbitrary radii. Intramolecular H-bond is illustrated by dashed line. b) ORTEP representation of L⁵. Displacement ellipsoids are drawn at the 30% probability level and H atoms are shown as small spheres of arbitrary radii. Intramolecular H-bond is illustrated by dashed line.

The C—N double bond is the most important indicators for Schiff base compounds. These bonds are 1.281(1) and 1.283(3) Å for L⁴ and L⁵, respectively. These values are in the expected range of Schiff base compounds [51].

There are two possible tautomeric forms for *o*-Hydroxy Schiff base ligands, the phenol-imine

(OH) and the ketoamine (NH) forms. The C9—N1 and C15—O3 bond distances of L⁴ and

L⁵ can be indicators of these tautomeric types. In ketoamine tautomer, C15—O3 bond is a double bond and C9—N1 is a single bond. While C15—O3 and C9—N1 bonds in phenol–imine tautomer are single bond and double bond, respectively [52]. Observation of single bond for C15—O3 (1.346(7) and 1.348(3) Å for L⁴ and L⁵, respectively) and double bond for C9—N1 (1.281(9) and 1.283(3) Å for L⁴ and L⁵, respectively) confirmed that both ligands (L⁴ and L⁵) are in phenol–imine form.

In both ligands N(1)⋯H(3)—O(3) intramolecular hydrogen bond between N atom and the OH group generates a S(6) motif that helps to stabilize the planarity of the molecule [51,52]. The intramolecular H-bond distances and angle are also in the expected range (O—H: 0.821 Å, H⋯N: 1.935 Å, N⋯O: 2.582 Å and N—H—O: 136.30° for L⁴ and O—H: 0.897 Å, H⋯N: 1.760 Å, N⋯O: 2.585 Å and N—H—O: 151.69° for L⁵) [48, 49]. The non-classical intermolecular H-bonds also are formed in both L⁴ and L⁵ ligands. There is a bifurcated (or three centered) hydrogen bond in each ligands (O1⋯H7—C7 and O1⋯H9—C9 in L⁴ and O1⋯H16A—C16 and O1⋯H16C—C16 in L⁵). In addition, O3 and O2 form intermolecular H-bonds in L⁴ and L⁵, respectively (O3⋯H13—C13, O3⋯H1A—C1 and O2⋯H1B—C1 in L⁴ and O3⋯H5—C5 and O2⋯H1A—C1 in L⁵) (Table 2). According to the hydrogen-bonding classification [53] these intramolecular and intermolecular hydrogen bonding are moderate and weak interactions, respectively.

Table 2. Intra- and intermolecular hydrogen bond geometries (Å,°) for L⁴ and L⁵.

	D—H⋯A	D—H	H⋯A	D⋯A	D—H⋯A	Empty Cell
L ⁴						
	O(3)—H(3)⋯N(1)	0.82	1.93	2.58	136	Moderate
	C(13)—H(13)⋯O(3)	0.93	2.68	3.42	137	Weak
	C(7)—H(7)⋯O(1)	0.93	2.61	3.29	130	Weak
	C(9)—H(9)⋯O(1)	0.93	2.51	3.41	163	Weak
	C(1)—H(1A)⋯O(3)	0.96	2.59	3.40	141	Weak

	D—H...A	D—H	H...A	D...A	D—H...A	Empty Cell
L⁵						
	O(3)—H(3)...N(1)	0.89	1.76	2.58	151	Moderate
	C(1)—H(1A)...O(2)	0.96	2.54	3.49	171	Weak
	C(16)—H(16A)...O(1)	0.96	2.43	3.33	155	Weak
	C(16)—H(16C)...O(1)	0.96	2.71	3.30	120	Weak

Table 3. Analytical and physical data of Schiff base ligands.

Compound	Empirical formula	Molecular weight	Color	Yield (%)
L¹	C ₁₄ H ₁₀ BrNO ₃	320.14	Yellow powder	83
L²	C ₁₄ H ₁₀ BrNO ₃	320.14	Yellow powder	80
L³	C ₁₅ H ₁₂ BrNO ₃	334.17	Yellow powder	85
L⁴	C ₁₇ H ₁₇ NO ₄	299.33	Red crystal	83
L⁵	C ₁₆ H ₁₅ NO ₄	285.29	Red crystal	81

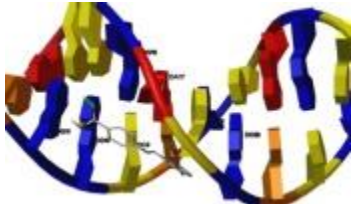
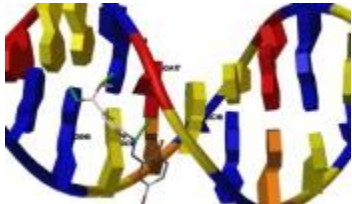
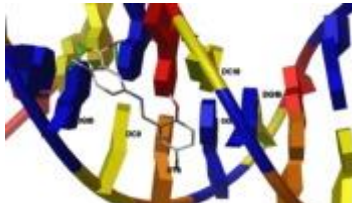
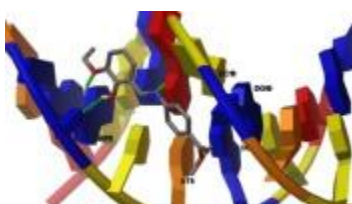
Table 4. Characteristic IR stretching bands of Schiff base ligands in cm⁻¹.

Compound	ν_{C-N}		ν_{as(COO⁻(carboxylate))}	ν_{s(COO⁻(carboxylate))}
	ν_C	N (azomethine)		
L¹	1279	1595	1680	1428
L²	1274	1619	1677	1421
L³	1279	1611	1683	1422
L⁴	1278	1591	1706	1455
L⁵	1261	1591	1721	1467

Table 5. The values of K_b , n , K_{sv} and k_q for binding of the ligands to FS-DNA.

Type of ligand	K_b (M^{-1})	N	K_{sv} (M^{-1})	k_q ($M^{-1}\cdot S^{-1}$)
L^1	8.9×10^4	0.45	4.1×10^3	4.1×10^{11}
L^2	6.8×10^4	0.42	3.2×10^3	3.2×10^{11}
L^3	1.2×10^5	0.28	5.6×10^3	5.6×10^{11}
L^4	2.3×10^5	0.24	3.1×10^3	3.1×10^{11}
L^5	1.7×10^5	0.34	5.3×10^3	5.3×10^{11}

Table 6. Binding energies and binding modes of the ligands during their interaction with DNA. (H-bond interactions are shown by green spheres).

Ligand	Binding Energy ($kcal\cdot mol^{-1}$)	K_b/M^{-1}	Type of interaction	Nucleotides in the binding site	Binding mode
L^1	-6.98	1.32×10^5	H-bond	DT8, DC9, DG10, DG11, DG16, DA17, DC18, DG19	
L^2	-6.94	1.23×10^5	H-bond	DC9, DG10, DG16, DA17, DC18	
L^3	-7.13	1.70×10^5	H-bond	DT8, DC9, DG10, DG11, DA17, DC18, DG19	
L^4	-7.34	2.42×10^5	H-bond	DT8, DC9, DG10, DG11, DA17, DC18, DG19	

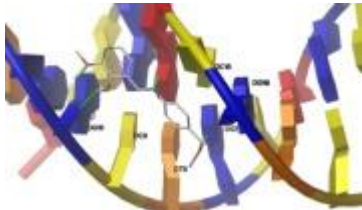
Ligand	Binding Energy (kcal·mol ⁻¹)	K _b /M ⁻¹	Type of interaction	Nucleotides in the binding site	Binding mode
L ⁵	-7.25	2.08 × 10 ⁵	H-bond	DG7, DT8, DC9, DG10, DG11, DA17, DC18, DG19	

Table 7. Mean RMSD values for free and conjugated DNA during 8 ns of MD simulation.

System	RMSD/nm
Free DNA	0.2279 ± 0.04
DNA-L ¹	0.2243 ± 0.04
DNA-L ²	0.2397 ± 0.06
DNA-L ³	0.2472 ± 0.04
DNA-L ⁴	0.3399 ± 0.06
DNA-L ⁵	0.1685 ± 0.05

3.4. Interaction with DNA

3.4.1. Absorption spectroscopic studies

The UV–Vis absorption spectroscopy is also a useful technique which has been frequently used to examine binding process. The photometric titration was carried out by adding various amount of FS-DNA to the ligands solutions in mole ratio range of [DNA]/[ligand] = 0–4.5 (Fig. S6). Generally, hyperchromic or hypochromic effect and red or blue shift are observed in the UV–Vis spectrum of a drug upon its DNA-binding [18]. Through addition of various amount of the FS-DNA, a hypochromic effect was observed in the ligands absorption spectra. These spectral changes suggest that the ligands can interact with FS-DNA through groove binding mode [54].

3.4.2. Fluorescence quenching experiments

EB is a standard intercalating agent of DNA that is used to study DNA-binding of compounds. A significant increase in fluorescence intensity of EB is observed upon addition of DNA, while EB shows a weak fluorescence emission in solution due to hydrogen transfer from one of its amino group into solution which causes non-radiative decay [[55], [56], [57], [58]]. Figs. 2 and S7,

show the fluorescence quenching of FS-DNA (4×10^{-4} M) at the presence of various amounts of the ligands (8×10^{-5} M). These ligands can displace EB by changing the DNA conformation. Consequently, the DNA-bound EB molecules are converted to their free form in solution and cause fluorescence quenching [19, 59].

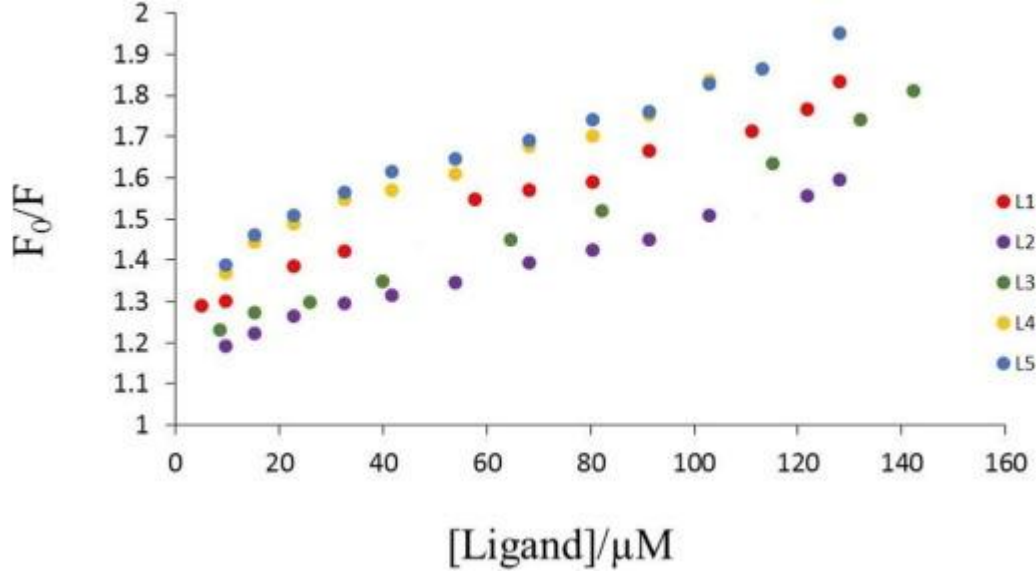


Fig. 2. Stern-Volmer plot for the synthesized ligands–DNA systems.

In order to determine the binding ability of the ligands, the Stern–Volmer quenching plot (Eq. (1)) was obtained by monitoring the fluorescence quenching of DNA-EB with increasing the concentration of the ligands [53].

$$\frac{F_0}{F} = 1 + K_{SV}[Q] = 1 + k_q \tau [Q] \quad (1)$$

where, F_0 and F are the fluorescence intensity of DNA-EB in the absence and presence of the ligands. K_{sv} is the Stern-Volmer quenching constant, k_q is the quenching rate constant of biomolecule, $[Q]$ is concentration of the quencher (complexes) and τ is the average lifetime of biomolecule without quencher (typically equal to 10^{-8} s for biomacromolecules) [18]. K_{sv} is determined from the plot of F_0/F vs. $[Q]$ (Fig. 2). The values of K_{sv} were presented in Table 5. There are two mechanisms for fluorescence quenching: static quenching and dynamic quenching. In the static mechanism, the fluorophore and the quencher collide together in the ground state, but the fluorophore and quencher collide together in the excited state in dynamic mechanism [18]. The Stern-Volmer plots indicate that fluorescence quenching may have only one of the above mechanisms or combination of them [54]. Our results showed that the plots are linear and therefore, the mechanism should be dynamic or static. The values of k_q were obtained for DNA (Table 5) and the values were about $10^{11} \text{ M}^{-1} \cdot \text{S}^{-1}$. This confirms that fluorescence quenching of biomolecule occurs by static mechanism since k_q values are greater than limiting diffusion rate constant of the diffusional quenching for biopolymers ($2 \times 10^{10} \text{ M}^{-1} \cdot \text{S}^{-1}$).

The binding constants (K_b) were determined using the following equation [54]:

$$\text{Ln} \left(\frac{F_0 - F}{F} \right) = \text{Ln} K_b + n \text{Ln} [Q] \quad (2)$$

“ K_b ” is obtained from the plot of $\text{Ln}((F_0 - F)/F)$ versus $\text{Ln}[Q]$ as y-intercept. These plots are present in Fig. 3. The K_b values (Table 5) reveal that the L^4 -DNA complex is more stable than the other compounds. Moreover, this result is in good agreement with the molecular docking results.

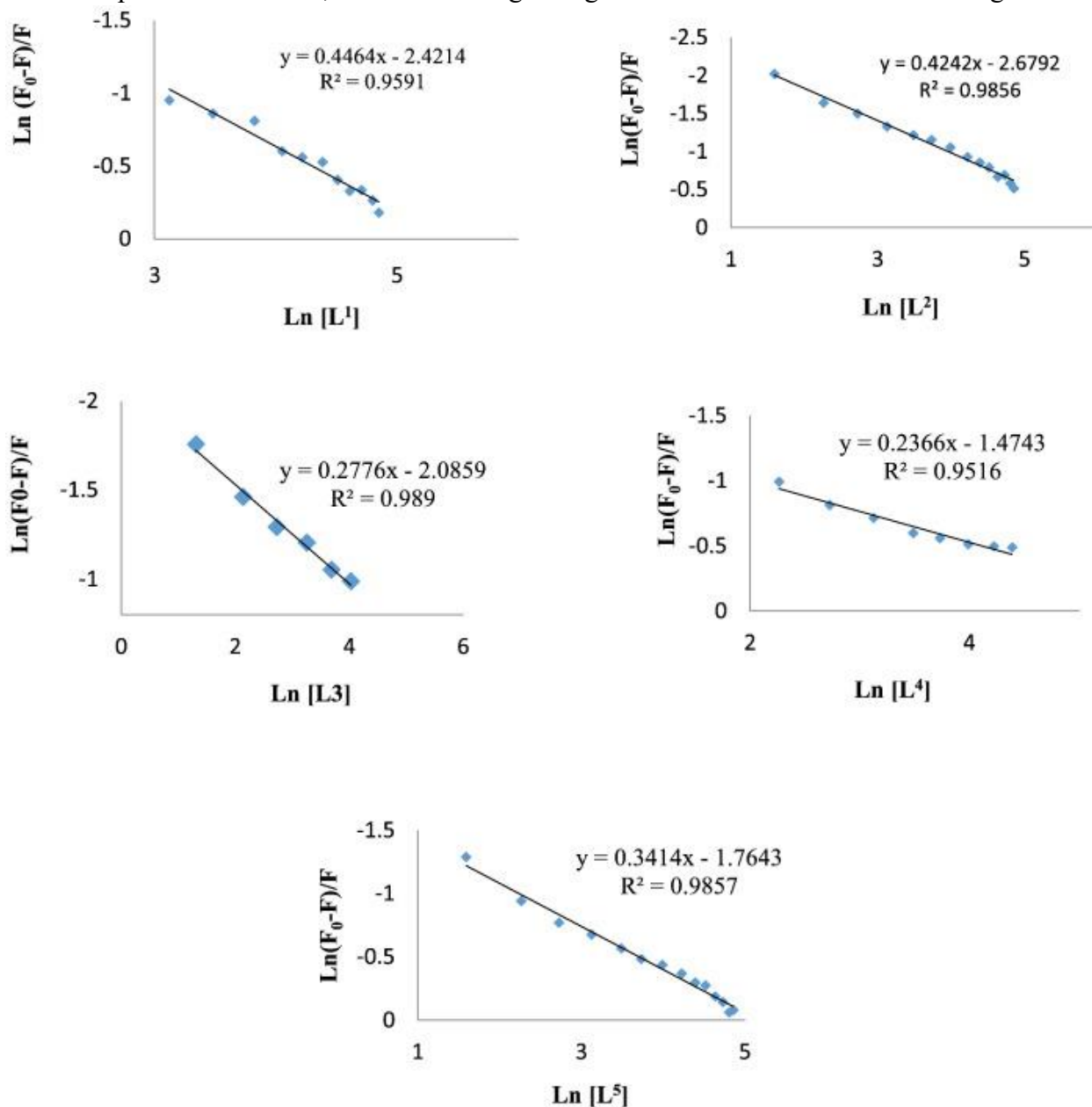


Fig. 3. Plot of $\text{Ln}(F_0 - F)/F$ vs. $\text{Ln}[\text{ligand}]$ for DNA-binding.

Based on the structural similarity of the ligands, they can be arranged in two groups: (i) L^1 , L^2 , L^3 and (ii) L^4 and L^5 . The comparison of L^1 , L^2 and L^3 shows that L^3 has the most affinity for FS-DNA. This difference can be due to existence of the electron donating group (methyl) on the phenyl ring of L^3 . Furthermore, all substituents in L^1 and L^2 are the same and they differ only in

the position of COOH on the phenyl ring. Hence, their DNA-binding constants have slight difference.

Moreover, L^4 has higher binding affinity to FS-DNA than L^5 . This indicates that the FS-DNA binding ability in this group of the synthesized ligands rises with increasing the electron donating ability of the substituent on their phenyl ring. This result is in good agreement with previous results for binding of DNA, protein to palladium(II) complexes [60, 61].

3.4.3. Cyclic voltammetry (CV) measurements

Cyclic voltammetry is one of the known methods to investigate the interaction of DNA with drugs. CV measurements were performed using an Autolab (PGSTAT 30), with a three-electrode system: a 0.10-cm-diameter Glassy carbon (GC) disc, a calomel electrode and a Pt wire as working, reference and counter electrodes, respectively.

L^4 ligand which has the most binding constant among the five synthesized Schiff base ligands, was chosen for cyclic voltammetry measurements. The supporting electrolyte was 50 mM of Tris-HCl buffer solution (pH = 7.4). The ligand and DNA concentrations were constant (5.0×10^{-5} M) and interaction time was 2 min. Fig. 4 shows the cyclic voltammograms of L^4 ligand in the absence and presence of DNA. The cathodic peak around -0.55 V in the curve can be attributed to the reduction peak of guanine oxidation intermediate [62]. This observation confirms that L^4 has appropriate interaction with DNA.

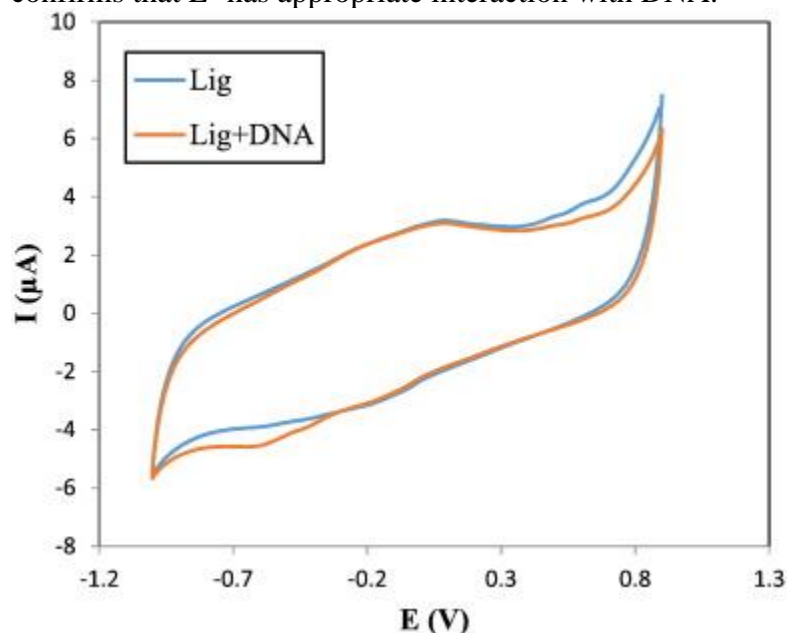


Fig. 4. Cyclic voltammetry of L^4 + DNA.

3.4.4. Circular dichroism (CD) spectroscopy

The CD spectra of DNA in free and bonded form to the L^4 ligand are shown in Fig. 5. The CD spectrum of free double stranded DNA exhibits three marker peaks at about 222 (positive), 245 (negative) and 280 nm (positive). The positive peak at about 280 nm due to base stacking and negative peak at 245 nm due to polynucleotide helicity are main peaks of DNA for its B-type, which are highly sensitive towards the DNA interaction with small molecules [63]. The L^4 ligand which showed the most binding constant with FS-DNA was selected for CD spectroscopy studies. Fig. 5 shows that the intensity of DNA peaks has been altered due to its interaction with

the L⁴ ligand. The results indicate that binding of the L⁴ ligand alters the DNA conformation. This observation is in consistent with the molecular dynamics (MD) simulation results (Section 3.4.6).

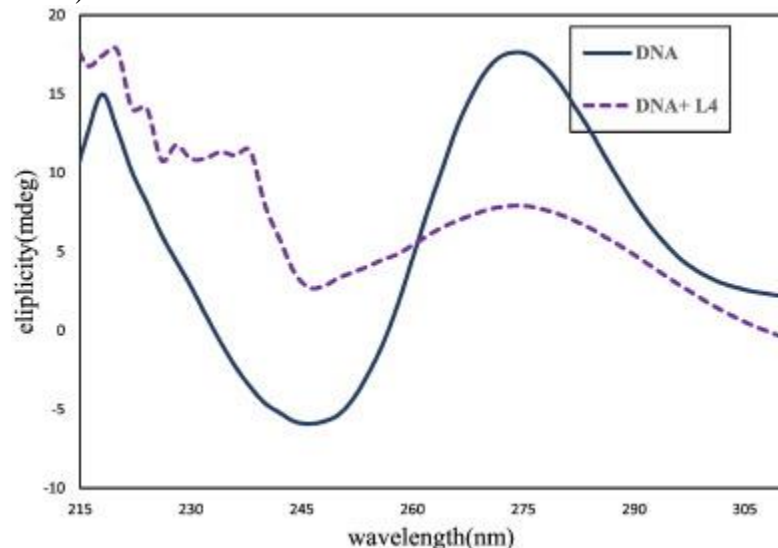


Fig. 5. The CD spectra of DNA in the absence and presence of L⁴ ligand in the molar ratio [L⁴]/[DNA] = 1.

3.4.5. Molecular docking studies

Molecular docking is a valuable technique to predict the stable structure of receptor-ligand complex for better recognition of the interaction details in drug discovery process. This method is frequently employed as virtual searching tools in primary steps of drug design and development. In order to find out the preferred location of the ligands on DNA, molecular docking studies were carried out. Table 6 represents the obtained binding modes and docking energies of the ligands during their interaction with DNA. The docked models suggest that the ligands bind with the minor groove of DNA with standard binding free energy (ΔG°) of -6.98 , -6.94 , -7.13 , -7.34 and -7.25 kcal.mol⁻¹ for L¹, L², L³, L⁴ and L⁵, respectively. These scores are related to the docking cluster with maximum population and minimum binding energy. These results are in good agreement with the obtained fluorescence results (see Section 3.4.2). Also, docking studies showed that H-bond interactions have the main role in the stability of ligand-DNA complexes.

3.4.6. Molecular dynamics (MD) simulation

The beginning structures for the MD analyses were selected from the conformations with the lowest docking energies. The stability of the systems (DNA and the ligands) properties was examined by means of RMS deviations (RMSD) of unbound and ligand conjugated DNA with respect to the initial structure and RMS fluctuations (RMSF) of atoms of the ligands. Preliminary simulations over 8 ns time were performed on DNA with the ligands. Table 7 provides the average values of RMSD for free and conjugated DNA. Fig. 6a indicates that the trajectories of both systems are stable and their RMSD reached equilibrium and fluctuated around its mean

value after about 1 ns simulation time. In addition, the RMSF values of the atomic positions of the ligands were calculated to examine their conformational variations (Fig. 6b). The results indicate that the ligands atoms showed limited fluctuations (<0.20 nm). Hence, it can be concluded that the interactions of DNA and the ligands were stable during the simulation time.

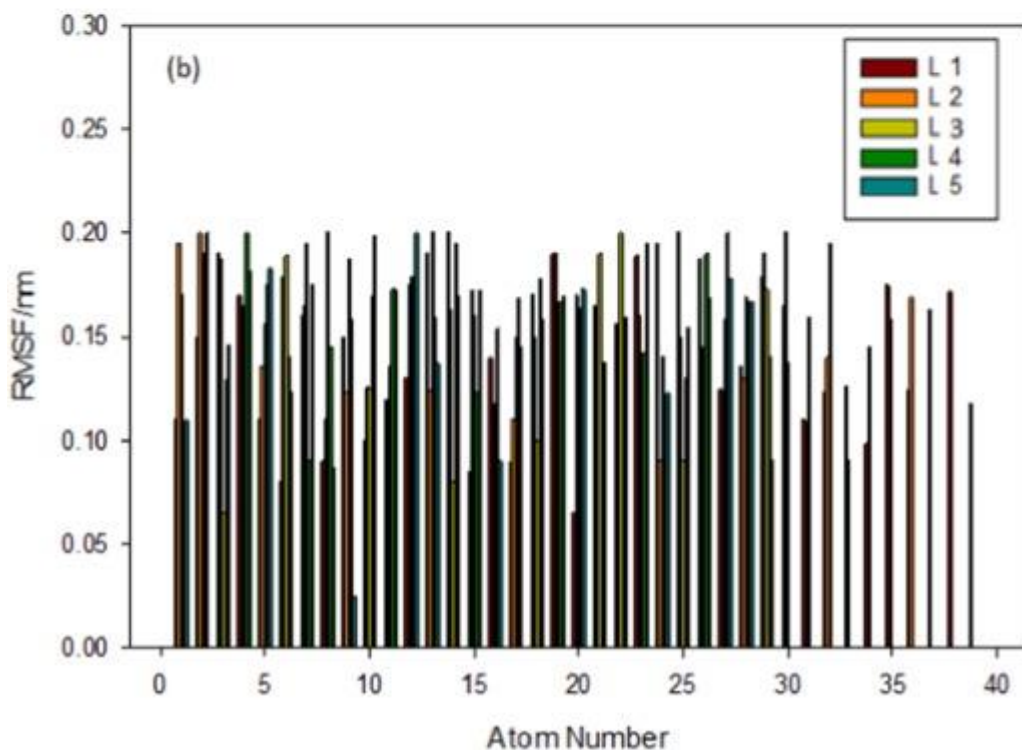
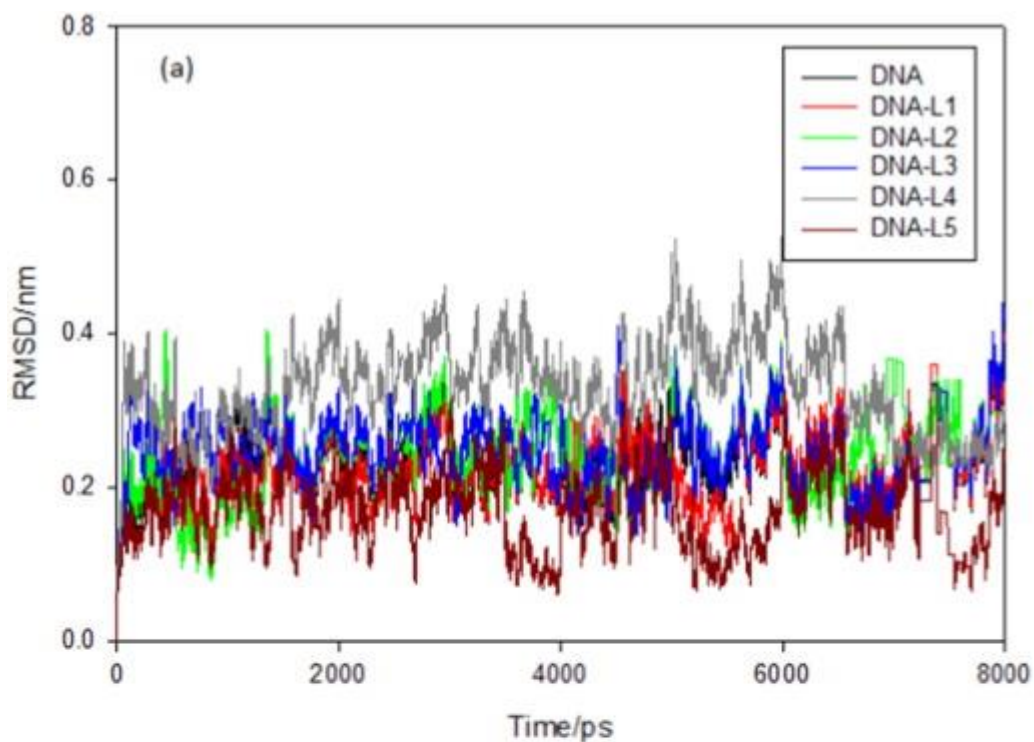


Fig. 6. a) Time dependence of RMS deviation of distance (RMSD) between atoms from the crystal structure as a function of simulation time for free DNA and conjugated DNA. b) Atomic fluctuations of the DNA conjugated Schiff base ligands during 8 ns of MD simulation.

4. Conclusion

In the current study, five novel Schiff base ligands containing hydroxyl groups were synthesized and characterized using IR, ^1H and ^{13}C NMR techniques. In addition, the structures of L^4 and L^5 were determined using single crystal X-ray method. DNA-binding of the ligands was investigated using fluorescence quenching, UV–Vis spectroscopy and cyclic voltammetry methods. Based on similarity of the ligands structures and their K_b values, their affinity for binding to FS-DNA follow as: $\text{L}^3 > \text{L}^1 > \text{L}^2$ and $\text{L}^4 > \text{L}^5$. Furthermore, the atomic details of ligands-DNA interactions were investigated using molecular docking and MD simulation methods. Molecular docking results show that all of the synthesized ligands are minor groove binders and H-bond interactions have dominant role in the stability of ligand-DNA complexes. Also, the MD results indicate that the interactions of DNA and the ligands were stable during the simulation time. All of the results indicate that the FS-DNA binding ability of the synthesized ligands rises with increasing the electron donating ability of the substituent on their phenyl ring. Also, both of the CD spectroscopy and MD simulation results (RMSD) show that Schiff base binding destabilizes DNA double helix.

Acknowledgement

The authors are grateful to the Research Council of the University of Isfahan for financial support of this work.

Appendix A. Supplementary data

CCDC 1549535 and 1549534 contain the supplementary crystallographic data for L^4 and L^5 , respectively. These data can be obtained free of charge via <http://www.ccdc.cam.ac.uk/conts/retrieving.html>, or from the Cambridge Crystallographic Data Centre, 12 Union Road, Cambridge CB2 1EZ, UK. Fax: +44 1223 336 033; or e-mail: deposit@ccdc.cam.ac.uk. Supplementary data associated with this article can be found in the online version, at <https://doi.org/10.1016/j.molliq.2018.01.029>.

References

- [1] M.H. Habibi, E. Askari, Synthesis, Structural Characterization, Thermal, and Electrochemical Investigations of a Square Pyramid Manganese (III) Complex with a Schiff Base Ligand Acting as N₂O₂ Tetradentate in Equatorial and as O Monodentate in Axial Positions: Application as a Precursor for Preparation of Mn-doped ZnO Nanoparticle, Synthesis and Reactivity in Inorganic, Metal-organic, and Nano-metal Chemistry, 43, 2013 406–411.
- [2] B. Hathaway, A. Tomlinson, Copper (II) ammonia complexes, Coord. Chem. Rev. 5 (1970) 1–43.
- [3] P. Jandera, M. Škavrada, L. Anděl, D. Komers, G. Guiochon, Description of adsorption equilibria in liquid chromatography systems with binary mobile phases, J. Chromatogr. A 908 (2001) 3–17.
- [4] A.M. Kadry, C.S. Okereke, M.S. Abdel-Rahman, M.A. Friedman, R.A. Davis, Pharmacokinetics

- of benzophenone-3 after oral exposure in male rats, *J. Appl. Toxicol.* 15 (1995) 97–102.
- [5] S. Kashanian, J. Ezzati Nazhad, Dolatabadi, *In vitro* study of calf thymus DNA interaction with butylated hydroxyanisole, *DNA Cell Biol.* 28 (2009) 535–540.
- [6] S. Kashanian, M.M. Khodaei, P. Pakravan, Spectroscopic studies on the interaction of isatin with calf thymus DNA, *DNA Cell Biol.* 29 (2010) 639–646.
- [7] S. Kumar, D.N. Dhar, P. Saxena, *Applications of Metal Complexes of Schiff Bases - A Review*, 2009.
- [8] N. Raman, S. Sobha, A. Thamarachelvan, A novel bioactive tyramine derived Schiff base and its transition metal complexes as selective DNA binding agents, *Spectrochim. Acta A Mol. Biomol. Spectrosc.* 78 (2011) 888–898.
- [9] P. Subbaraj, A. Ramu, N. Raman, J. Dharmaraja, Novel mixed ligand complexes of bioactive Schiff base (E)-4-(phenyl (phenylimino) methyl) benzene-1, 3-diol and 2-aminophenol/2-aminobenzoic acid: synthesis, spectral characterization, antimicrobial and nuclease studies, *Spectrochim. Acta A Mol. Biomol. Spectrosc.* 117 (2014) 65–71.
- [10] N. Raman, S. Thalamuthu, J. Dhiveethuraja, M. Neelakandan, S. Banerjee, DNA cleavage and antimicrobial activity studies on transition metal (II) complexes of 4-aminoantipyrene derivative, *J. Chil. Chem. Soc.* 53 (2008) 1439–1443.
- [11] N. Raman, S. Thalamuthu, J. Dhiveethuraja, M. Neelakandan, S. Banerjee, DNA cleavage and antimicrobial activity studies on transition metal (II) complexes of 4-aminoantipyrene derivative, *J. Chil. Chem. Soc.* 53 (2008) 1439–1443.
- [12] A. Osowole, R. Kempe, R. Schobert, Synthesis, spectral, thermal, *in-vitro* antibacterial and anticancer activities of some metal (II) complexes of 3-(1-(4-methoxy-6-methyl)-2-pyrimidinylimino) methyl-2-naphthol, *Int. Res. J. Pure Appl. Chem.* 2 (2012) 105–129.
- [13] N. Shahabadi, S. Kashanian, F. Darabi, DNA binding and DNA cleavage studies of a water soluble cobalt (II) complex containing dinitrogen Schiff base ligand: the effect of metal on the mode of binding, *Eur. J. Med. Chem.* 45 (2010) 4239–4245.
- [14] A. Jayamani, N. Sengottuvelan, G. Chakkaravarthi, Synthesis, structural, electrochemical, DNA interaction, antimicrobial and molecular docking studies on dimeric copper (II) complexes involving some potential bidentate ligands, *Polyhedron* 81 (2014) 764–776.
- [15] A.-E. Radi, A.-E. El-Naggar, H.M. Nassef, Electrochemical and spectral studies on the interaction of the antiparasitic drug nitazoxanide with DNA, *Electrochim. Acta* 129 (2014) 259–265.
- [16] M.T. Behnamfar, H. Hadadzadeh, J. Simpson, F. Darabi, A. Shahpiri, T. Khayamian, M. Ebrahimi, H.A. Rudbari, M. Salimi, Experimental and molecular modeling studies of the interaction of the polypyridyl Fe (II) and Fe (III) complexes with DNA and BSA, *Spectrochim. Acta A Mol. Biomol. Spectrosc.* 134 (2015) 502–516.
- [17] C. Ozluer, H.E.S. Kara, *In vitro* DNA binding studies of anticancer drug idarubicin using spectroscopic techniques, *J. Photochem. Photobiol. B Biol.* 138 (2014) 36–42.
- [18] Z. Kazemi, H.A. Rudbari, M. Sahihi, V. Mirkhani, M. Moghadam, S. Tangestaninejad, I. Mohammadpoor-Baltork, G. Azimi, S. Gharaghani, A.A. Kajani, Synthesis, characterization and separation of chiral and achiral diastereomers of Schiff base Pd (II) complex: a comparative study of their DNA- and HSA-binding, *J. Photochem. Photobiol. B*

Biol. 163 (2016) 246–260.

[19] Z. Kazemi, H.A. Rudbari, M. Sahihi, V. Mirkhani, M. Moghadam, S. Tangestaninejad, I. Mohammadpoor-Baltork, S. Gharaghani, Synthesis, characterization and biological application of four novel metal-Schiff base complexes derived from allylamine and their interactions with human serum albumin: experimental, molecular docking and ONIOM computational study, *J. Photochem. Photobiol. B Biol.* 162 (2016) 448–462.

[20] I. Khosravi, F. Hosseini, M. Khorshidifard, M. Sahihi, H.A. Rudbari, Synthesis, characterization, crystal structure and HSA binding of two new N, O, O-donor Schiff-base ligands derived from dihydroxybenzaldehyde and tert-butylamine, *J. Mol. Struct.* 1119 (2016) 373–384.

[21] H. Yamada, M. Kojo, T. Nakahara, K. Murakami, T. Kakima, H. Ichiba, T. Yajima, T. Fukushima, Development of a fluorescent chelating ligand for scandium ion having a Schiff base moiety, *Spectrochim. Acta A Mol. Biomol. Spectrosc.* 90 (2012) 72–77.

[22] S. Cie, Program for the Acquisition and Analysis of Data XeAREA, Version 1, 30, Stoe & Cie GmbH, Darmstadt, Germany, 2005.

[23] X-RED, in: S.C. GmbH (Ed.), Program for Data Reduction and Absorption Correction, 2005 (Darmstadt, Germany).

[24] C. Stoe, X-SHAPE, Version 2.05, Program for Crystal Optimization for Numerical Absorption

Correction, Stoe & Cie GmbH, Darmstadt, Germany, 2004.

[25] G.M. Sheldrick, A short history of SHELX, *Acta Crystallogr. A: Found. Crystallogr.* 64 (2008) 112–122.

[26] M. Reichmann, S. Rice, C. Thomas, P. Doty, A further examination of the molecular weight and size of desoxypentose nucleic acid, *J. Am. Chem. Soc.* 76 (1954) 3047–3053.

[27] K. Zheng, F. Liu, X.-M. Xu, Y.-T. Li, Z.-Y. Wu, C.-W. Yan, Synthesis, structure and molecular

docking studies of dicopper (II) complexes bridged by N-phenolato-N'-[2-

(dimethylamino) ethyl] oxamide: the influence of terminal ligands on cytotoxicity and reactivity towards DNA and protein BSA, *New J. Chem.* 38 (2014) 2964–2978.

[28] X.-B. Fu, D.-D. Liu, Y. Lin, W. Hu, Z.-W. Mao, X.-Y. Le, Water-soluble DNA minor groove binders as potential chemotherapeutic agents: synthesis, characterization, DNA binding and cleavage, antioxidation, cytotoxicity and HSA interactions, *Dalton Trans.* 43 (2014) 8721–8737.

[29] F. Arjmand, A. Jamsheera, D. Mohapatra, Synthesis, characterization and in vitro DNA binding and cleavage studies of Cu (II)/Zn (II) dipeptide complexes, *J. Photochem. Photobiol. B Biol.* 121 (2013) 75–85.

[30] P. Fromherz, B. Rieger, Photoinduced electron transfer in DNA matrix from intercalated ethidium to condensed methylviologen, *J. Am. Chem. Soc.* 108 (1986) 5361–5362.

[31] X.-B. Fu, G.-T. Weng, D.-D. Liu, X.-Y. Le, Synthesis, characterization, DNA binding and cleavage, HSA interaction and cytotoxicity of a new copper (II) complex derived from 2-(2'-pyridyl) benzothiazole and glycylglycine, *J. Photochem. Photobiol. A Chem.* 276 (2014) 83–95.

- [32] M. Waring, Complex formation between ethidium bromide and nucleic acids, *J.Mol. Biol.* 13 (1965) 269–282.
- [33] M.-Y. Tian, X.-F. Zhang, L. Xie, J.-F. Xiang, Y.-L. Tang, C.-Q. Zhao, The effect of Cu²⁺ on the interaction between an antitumor drug—mitoxantrone and human serum albumin, *J. Mol. Struct.* 892 (2008) 20–24.
- [34] M. Khorshidifard, H.A. Rudbari, Z. Kazemi-Delikani, V. Mirkhani, R. Azadbakht, Synthesis, characterization and X-ray crystal structures of Vanadium (IV), Cobalt (III), Copper (II) and Zinc (II) complexes derived from an asymmetric bidentate Schiffbase ligand at ambient temperature, *J. Mol. Struct.* 1081 (2015) 494–505.
- [35] C.N. Pace, F. Vajdos, L. Fee, G. Grimsley, T. Gray, How to measure and predict the molar absorption coefficient of a protein, *Protein Sci.* 4 (1995) 2411–2423.
- [36] M. Reichmann, S. Rice, C. Thomas, P. Doty, A further examination of the molecular weight and size of desoxypentose nucleic acid, *J. Am. Chem. Soc.* 76 (1954) 3047–3053.
- [37] G.M. Morris, D.S. Goodsell, R.S. Halliday, R. Huey, W.E. Hart, R.K. Belew, A.J. Olson, Automated docking using a Lamarckian genetic algorithm and an empirical binding free energy function, *J. Comput. Chem.* 19 (1998) 1639–1662.
- [38] H.J. Berendsen, D. van der Spoel, R. van Drunen, A message-passing parallel molecular dynamics implementation, *Comput. Phys. Commun.* 91 (1995) 43–56.
- [39] A. Pérez, I. Marchán, D. Svozil, J. Spöner, T.E. Cheatham, C.A. Laughton, M. Orozco, Refinement of the AMBER force field for nucleic acids: improving the description of α/γ conformers, *Biophys. J.* 92 (2007) 3817–3829.
- [40] J. Wang, R.M. Wolf, J.W. Caldwell, P.A. Kollman, D.A. Case, Development and testing of a general amber force field, *J. Comput. Chem.* 25 (2004) 1157–1174.
- [41] A. Frisch, Gaussian 03. U. User's Reference: Manual Version 7.1 (Corresponding to Gaussian 03 Revision D. 1): Gaussian, 2005.
- [42] C. Lee, W. Yang, R.G. Parr, Development of the Colle-Salvetti correlation-energy formula into a functional of the electron density, *Phys. Rev. B* 37 (1988) 785.
- [43] A.W.S. da Silva, W.F. Vranken, ACPYPE-Antechamber python parser interface, *BMC Res. Notes* 5 (2012) 367.
- [44] W.L. Jorgensen, J. Chandrasekhar, J.D. Madura, R.W. Impey, M.L. Klein, Comparison of simple potential functions for simulating liquid water, *J. Chem. Phys.* 79 (1983) 926–935.
- [45] P. Mark, L. Nilsson, Structure and dynamics of the TIP3P, SPC, and SPC/E water models at 298 K, *J. Phys. Chem. A* 105 (2001) 9954–9960.
- [46] M. Parrinello, A. Rahman, Polymorphic transitions in single crystals: a new molecular dynamics method, *J. Appl. Phys.* 52 (1981) 7182–7190.
- [47] A. Rahman, F.H. Stillinger, Molecular dynamics study of liquid water, *J. Chem. Phys.* 55 (1971) 3336–3359.
- [48] A. Lemak, N. Balabaev, On the Berendsen thermostat, *Mol. Simul.* 13 (1994) 177–187.
- [49] T. Darden, D. York, L. Pedersen, Particle-mesh Ewald: an $N \cdot \log(N)$ method for Ewald sums in large systems, *J. Chem. Phys.* 98 (1993) 10089–10092.
- [50] U. Essmann, L. Perera, M.L. Berkowitz, T. Darden, H. Lee, L.G. Pedersen, A smooth particle mesh Ewald method, *J. Chem. Phys.* 103 (1995) 8577–8593.

- [51] I. Khosravi, F. Hosseini, M. Khorshidifard, M. Sahihi, H.A. Rudbari, Synthesis, characterization, crystal structure and HSA binding of two new N, O, O-donor Schiff-base ligands derived from dihydroxybenzaldehyde and tert-butylamine, *J. Mol. Struct.* 1119 (2016) 373–384.
- [52] A. Özek, Ç. Albayrak, M. Odabaşoğlu, O. Büyükgüngör, Three (E)-2-[(bromophenyl)iminomethyl]-4-methoxyphenols, *Acta Crystallogr. Sect. C: Cryst. Struct. Commun.* 63 (2007) o177–o180.
- [53] T. Steiner, The hydrogen bond in the solid state, *Angew. Chem. Int. Ed.* 41 (2002) 48–76.
- [54] Z. Kazemi, H.A. Rudbari, V. Mirkhani, M. Sahihi, M. Moghadam, S. Tangestaninejad, I. Mohammadpoor-Baltork, Synthesis, characterization, crystal structure, DNA- and HSA-binding studies of a dinuclear Schiff base Zn (II) complex derived from 2-hydroxynaphthaldehyde and 2-picolyamine, *J. Mol. Struct.* 1096 (2015) 110–120.
- [55] F. Arjmand, A. Jamsheera, D. Mohapatra, Synthesis, characterization and in vitro DNA binding and cleavage studies of Cu (II)/Zn (II) dipeptide complexes, *J. Photochem. Photobiol. B Biol.* 121 (2013) 75–85.
- [56] X.-B. Fu, G.-T. Weng, D.-D. Liu, X.-Y. Le, Characterization, DNA binding and cleavage, HSA interaction and cytotoxicity of a new copper (II) complex derived from 2-(2-pyridyl) benzothiazole and glycylglycine, *J. Photochem. Photobiol. A Chem.* 276 (2014) 83–95.
- [57] M. Waring, Complex formation between ethidium bromide and nucleic acids, *J. Mol. Biol.* 13 (1965) 269–282.
- [58] P. Fromherz, B. Rieger, Photoinduced electron transfer in DNA matrix from intercalated ethidium to condensed methylviologen, *J. Am. Chem. Soc.* 108 (1986) 5361–5362.
- [59] E. Pahonțu, D.-C. Ilieș, S. Shova, C. Paraschivescu, M. Badea, A. Gulea, T. Roșu, Synthesis, characterization, crystal structure and antimicrobial activity of copper (II) complexes with the Schiff base derived from 2-hydroxy-4-methoxybenzaldehyde, *Molecules* 20 (2015) 5771–5792.
- [60] P. Kalaivani, R. Prabhakaran, F. Dallemer, P. Poornima, E. Vaishnavi, E. Ramachandran, V.V. Padma, R. Renganathan, K. Natarajan, DNA, protein binding, cytotoxicity, cellular uptake and antibacterial activities of new palladium (II) complexes of thiosemicarbazone ligands: effects of substitution on biological activity, *Metallomics* 4 (2012) 101–113.
- [61] P. Kalaivani, R. Prabhakaran, E. Ramachandran, F. Dallemer, G. Paramaguru, R. Renganathan, P. Poornima, V.V. Padma, K. Natarajan, Influence of terminal substitution on structural, DNA, protein binding, anticancer and antibacterial activities of palladium (II) complexes containing 3-methoxy salicylaldehyde-4 (N) substituted thiosemicarbazones, *Dalton Trans.* 41 (2012) 2486–2499.
- [62] B.T. Psciuk, H.B. Schlegel, Computational prediction of one-electron reduction potentials and acid dissociation constants for guanine oxidation intermediates and products, *J. Phys. Chem. B* 117 (2013) 9518–9531.
- [63] M. Dehkhodaei, M. Sahihi, H.A. Rudbari, S. Gharaghani, R. Azadbakht, S. Taheri, A.A. Kajani, Studies of DNA- and HSA-binding properties of new nano-scale green synthesized Ni (II) complex as anticancer agent using spectroscopic methods, viscosity

measurement, molecular docking, MD simulation and QM/MM, *J. Mol. Liq.* 248 (2017) 24–35.